expression (12b). As is seen from the figure, for the receiver $t \geq 10$ sec the agreement of the relations can be regarded as satisfactory.

Thus, the results obtained above allow us to carry out an estimate of the speed of response of HRMC from below, their dynamic properties with the basic thermophysical and geometric parameters of the receivers being taken into account.

The results obtained in the paper can be used to calculate cooling systems of gas-discharge pipes, solid-body active media, and regenerators.

NOTATION

HRMC, heat receiver with a moving heat carrier; c, specific heat capacity of liquid heat carrier; v, volumetric flow rate of heat carrier; γ, density of heat carrier; C_m, heat capacity of heat-conducting material of HRMC; C_l, heat capacity of heat carrier; α, coefficient of heat transfer at the heat-conducting material–heat carrier interface; A, absorption coefficient of HRMC; a^2, coefficient of thermal diffusivity of heat-conducting material; k, coefficient of thermal conductivity of the heat-conducting material; b, l, m, length, width, and thickness of the heat-conducting material of HRMC; β, interaction parameter; p, complex variable; $T(x, t)$, $U(x, t)$, functions describing the variation of temperature of the heat carrier and of temperature of the heat-conducting material along the direction of propagation of the flow with time; $T_0(t)$, $T_e(t)$, functions describing the variation of temperature, respectively, at the entry and at the exit of HRMC; $N(x, t)$, radiation power absorbed by the receiver, referred to unit length; $P(t)$, radiation power absorbed by the receiver; $T(p)$, $U(p)$, $N(p)$, functions $T(x, t)$, $U(x, t)$, $N(x, t)$ transformed according to Laplace; $T_0(p)$, $T_e(p)$, $P(p)$ transforms of the functions $T_0(t)$, $T_e(t)$, $P(t)$, transformed according to Laplace.

LITERATURE CITED

1. R. A. Valitov and V. N. Sretenskii, Radio Measurements at Ultra-High-Frequencies [in Russian], Voenizdat, Moscow (1958).
2. E. I. Ivlev, Tr. Metrolog. Inst., 150, No. 90, 12 (1967).
3. E. I. Ivlev, Inzh.-Fiz. Zh., 23, No. 2 (1972).
4. E. I. Ivlev and A. V. Kubarev, Tr. Metrolog. Inst., 172, No. 112, 44 (1974).

INVESTIGATION OF THE THERMOPHYSICAL CHARACTERISTICS OF CRYOGENIC HEAT PIPES WITH A METAL-FIBER WICK

M. G. Semena and A. I. Levterov

UDC 536.27:536.248.2

Results are presented of an experimental investigation of the maximum heat-transmission capability and the heat-transfer intensity characteristics in the heat input and heat output of cyrogenic heat pipes.

The reliability of efficient and compact heat-transfer devices of the heat-pipe type ensure that they are widely used in practice over the whole technically available temperature range, including the cryogenic range [1-4]. An analysis of experimental and theoretical investigations [1-7] shows that the primary feature for efficient operation of cryogenic heat pipes is choice of the heat structure for the heat pipe, since the characteristic parameter $N=\sigma r/\nu$ and the thermal conductivity of cryogenic liquids are significantly lower than for low-temperature liquids (water, alcohol, or acetone). Therefore, metal-fiber wicks [8] can be regarded as one of the most promising capillary-porous structures for heat pipes in liquid nitrogen. The technology for manufacture of metal-fiber structures from monodiscrete fibers of a specific length is such that one can reduce to a minimum the thermal contact resistance between the wall and the wick and can substantially increase

Kiev Polytechnic Institute.

Translated from Inzhenerno-Fizicheskii Zhurnal, Vol. 35, No. 1, pp. 48-53, July, 1978. Original article submitted June 15, 1977.

0022-0841/78/3501-0797$07.50

TABLE 1. Structural Characteristics of the Heat Pipes

Characteristics	Heat pipe		
	No. 1	No. 2	No. 3
Material of shell and wick	Copper	1Kh18N10T	1Kh18N10T
Outer shell diameter d, mm	8	10	38
Shell-wall thickness s, mm	1	1	2,5
Heat-pipe length L, mm	220	500	100
Heater zone length L_h, mm	60	80	50
Condensation zone length L_c, mm	60	120	40
Wick thickness δ_w, mm	0,45	1,0	1,35
Porosity II, %	82,0	75	70
Permeability K_w, m^2	$7 \cdot 10^{-11}$	$7 \cdot 10^{-11}$	$5 \cdot 10^{-11}$
Effective pore size D_{eff}, m	$68 \cdot 10^{-6}$	$60 \cdot 10^{-6}$	$50 \cdot 10^{-6}$

the thermal conductivity of the wick, saturated with liquid nitrogen (e.g., for a copper wick of porosity 75-80%, λ_{eff} = 12-8 W/m · °K). In regard to transport characteristics (permeability and capillary head), metal-fiber wicks are also interesting because of the high open porosity (II = 70-95%) for low values of the effective pore size (D_{eff} = 20-200 μm).

This paper presents some results of an experimental investigation of thermophysical characteristics of heat pipes in nitrogen. Three heat pipes were investigated, each having a shell of circular section with a metal-fiber wick welded to the inner surface. The geometric, structural, and also some other characteristics of the tested heat pipes and wicks are given in Table 1.

The filling of the heat pipes with the working liquid and the investigation were carried out on an experimental equipment designed along conventional lines [5]. Particular attention was paid to the accuracy in measuring the thermo-emf of the thermocouples, and the heat-flux supplied, and to setting the inclination of the heat pipe. The experimental technique was as follows.

For a specific amount of working liquid and a specific value of the heat-pipe inclination, the heat flux supplied was varied up to a value which produced a sharp increase in the wall temperature at the extreme section of the heat-supply zone. The measurements were made after steady heat-transfer conditions were established. From these measurements we determined the limiting heat flux Q_{max} and the temperature fields as a function of the amount of filling of heat-transfer agent and the inclination. Heat pipes Nos. 1 and 2, which operated horizontally, were filled in steps with working liquid, beginning from a theoretical value up to a certain excess of heat-transfer agent, for which the growth in the maximum heat-transfer capability of the heat pipes was observed to stop. The inclination of the heat pipes to the horizontal plane was set at various values. For example, for heat pipe No. 1 the range was $-10° \leq \varphi \leq +10°$, where the + refers to the condition when the evaporator was located above the condenser. The filling with heat-transfer agent during operation of this pipe in the inclined position was carried out with an excess of 0.1 g (when the design amount of heat-transfer agent was $\Omega = 1.2$ g).

The primary result of the experiment was obtaining the temperature distribution along the heat pipes for variation of the heat load, the amount of liquid poured in, and the inclination of the heat pipes. The temperatures were measured by 10-15 copper–Constantan thermocouples, welded to the heat-pipe surface in milled channels of depth 0.5 mm. Of these, four were located in the heat-supply zone, and the remainder in the heat-transfer and heat-removal zones. Figure 1 shows a typical location of thermocouples and the characteristic temperature distribution at the outer wall surface of heat pipe No. 1. At a certain value of heat load supplied, the temperature at the extreme section of the heater zone increased sharply, this being evidence of the onset of the heat-transmission-capability limit for the heat pipe (curve 4, points a). It is clear that the limiting heat flux Q_{max} is due to a limit in the transport characteristics of the wick and the thermophysical properties of the working liquid. This is confirmed by comparing these conditions with conditions at the same load, but at an inclination of $\varphi = -5°$ (curve 4, points b).

The onset of the limiting heat-transfer capacity of the heat pipes was determined from measurements of the dependence of temperature at the extreme section of the heat supply zone on the heat-flux supply (Fig. 2). The point of inflection of the curve fixes the value of the limiting heat flux for a certain filling of the heat-transfer agent and a certain heat-pipe inclination.

Values of maximum heat flux transmitted by the tested heat pipes in the horizontal position with the design filling of heat-transfer agent were estimated using the relation obtained from the premises quoted in [10]:

$$Q_{max} = 4 \frac{\sigma r}{\nu} \frac{K_w}{D_{eff}} \frac{F_w}{0{,}5(L_c + L_h) + L_t}. \quad (1)$$

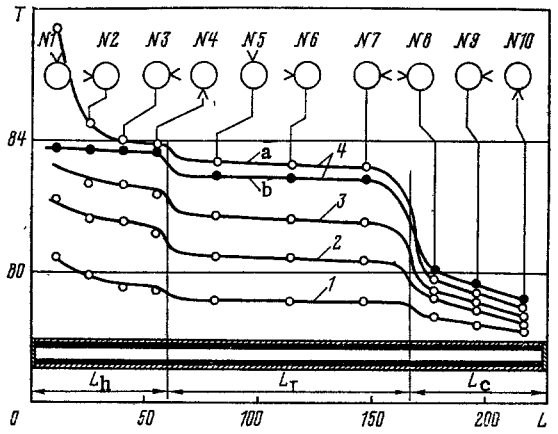

Fig. 1. Location of thermocouples on the surface of heat pipe No. 1 and the temperature distribution T, (°K) along the length L, mm: $\varphi = 0$, $\Omega = 1.6$ g; b) $\varphi = -5°$, $\Omega = 1.3$ g; 1) Q = 2 W; 2) 4; 3) 6; 4) 8 W.

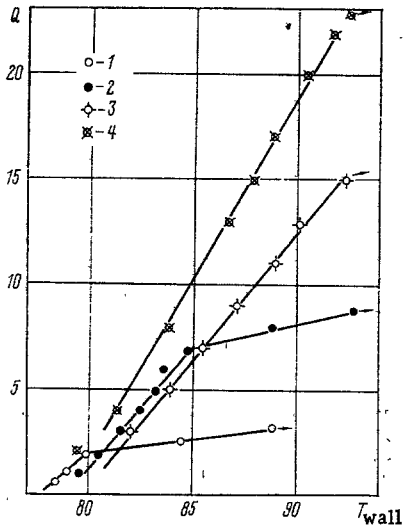

Fig. 2. Wall temperatures T_{wall} (°K) at the extreme section of the heat supply zone of heat pipes No. 1 as a function of the heat load supplied Q (W): 1) $\varphi = 0°$, $\Omega = 1.2$ g; 2) $\varphi = 0°$, $\Omega = 1.6$ g; 3) $\varphi = 0°$, $\Omega = 2.0$ g; 4) $\varphi = -5°$, $\Omega = 1.3$ g.

Calculations using Eq. (1) showed that only for pipe No. 3 does the maximum heat flux differ appreciably from the experimental value (for heat pipe No. 1, $Q^{t}_{max} = 1.95$ W, and $Q^{ex}_{max} = 2$ W; for No. 2 the values are 3.5 W and 5 W; for No. 3 the values are 72 W and 36 W). These discrepancies are evidently due to the fact that for heat pipes of large diameter, commensurate with the height of the capillary rise, when calculating Q_{max} one should take into account incomplete saturation of the wick with liquid in the upper part of the heat pipe; i.e., in Eq. (1) one must replace K_w and F_w by $K_w = f(h)$ and $F_w = f(h)$, where h is the height, computed from the lowest generator of the pipe.

From Fig. 2 (points 1, 2, and 3) one can see that for $\varphi = 0$ the limiting heat flux increases with increase in the excess of liquid arriving in unit active volume of the porous structure of the wick ($\Delta\Omega/V_{w\Pi}$). This is due to a reduction in the length of filtration of the heat-transfer agent in the heater zone. However, here the total temperature drop along the heat-pipe length increases, since the excess of working liquid acts as an additional thermal resistance in the condensation zone, where the wick saturated with liquid nitrogen makes the main contribution to the total thermal resistance of the heat pipe. The excess of heat-transfer agent is also undesirable when heat pipes operate against gravity forces $\varphi > 0$ and in weightless conditions, since it decreases the area of the active condensation zone. In the general case, overfilling with heat-transfer agent creates additional difficulties in maintaining cryogenic heat pipes at the conditions of the surrounding environment.

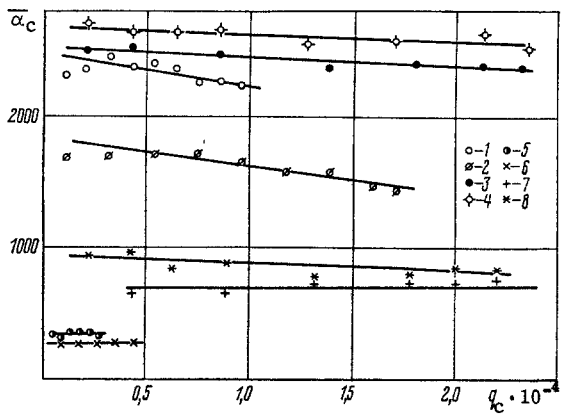

Fig. 3

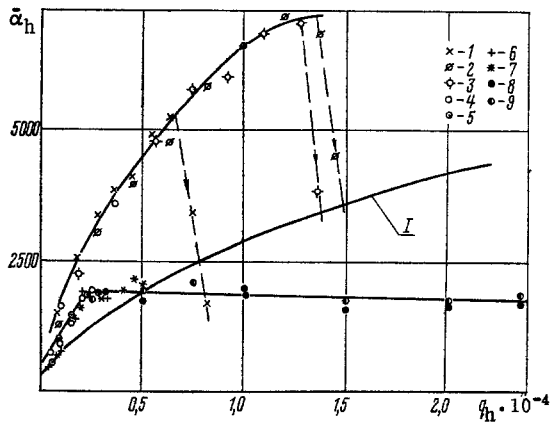

Fig. 4

Fig. 3. The average heat-transfer coefficient in the condensation zone of the heat pipes, $\bar{\alpha}_c$, W/m^2·°K as a function of the density of heat flux removed q_c (W/m^2): 1-4) heat pipe No. 1; 5-8) heat pipe No. 2; 1) $\Omega = 1.6$ g; $\varphi = 0$; 2) $\Omega = 2.0$ g, $\varphi = 0$; 3) $\Omega = 1.3$ g, $\varphi = -5°$; 4) $\Omega = 1.3$ g, $\varphi = -10°$; 5) $\Omega = 6.5$ g, $\varphi = 0$; 6) $\Omega = 9$ g, $\varphi = 0$; 7) $\Omega = 6.5$ g, $\varphi = -5°$; 8) $\Omega = 6.5$ g, $\varphi = -10°$.

Fig. 4. The average heat-transfer coefficient in the heat-supply zone of the heat pipes, $\bar{\alpha}_h$, (W/m^2·°K) as a function of the heat-flux density supplied, q_h (W/m^2): 1-3) heat pipe No. 1; 4-9) heat pipe No. 2; 1) $\Omega = 1.6$ g, $\varphi = 0$; 2) $\Omega = 2.0$ g, $\varphi = 0$; 3) $\Omega = 1.2$ g, $\varphi = 0$; 4) $\Omega = 6.1$ g, $\varphi = 0$; 5) $\Omega = 6.5$ g, $\varphi = 0$; 6) $\Omega = 7$ g, $\varphi = 0$; 7) $\Omega = 9$ g, $\varphi = 0$; 8) $\Omega = 6.5$ g, $\varphi = -5°$; 9) $\Omega = 6.5$ g, $\varphi = -10°$. I) The Kutateladze formula.

Figure 3 shows the average heat-transfer coefficient $\bar{\alpha}_c$ in the condensation zone as a function of the density of heat flux removed for various filling levels of working liquid and various inclination angles of heat pipes Nos. 1 and 2. In practice, the average heat-transfer coefficient in the heat-removal zone varies insignificantly with increase in the density of heat flux removed, but it depends strongly on the filling level of heat-transfer agent and on the inclination, which affects the saturation of the wick in the condensation zone and the thickness of the liquid layer in the lower part of the pipe section. The data obtained on average heat-transfer coefficients in the heat-removal zone are in good agreement with data of investigations on the thermal conductivity of the housing and the effective thermal conductivity of saturated metal-fiber wicks [9], if one takes into account that there is constantly a film of condensing liquid nitrogen on the surface of fibers facing toward the vapor channel. This is confirmed by comparing experimental and theoretical values of the coefficients $\bar{\alpha}_c$. In an experiment for heat pipe No. 2, $\bar{\alpha}_c = 0.35$ W/m^2·°K, and the theoretical value (in terms of an equivalent wick thickness and its effective thermal conductivity) is $\bar{\alpha}_c^{eq} = 0.55$ W/m^2·°K; i.e., there is an additional thermal resistance in the form of a liquid film on the metal-fiber surface, and it would require additional experiments to determine the film thickness accurately.

A comparison of the nature of the variation of the average heat-transfer coefficient as a function of the density of heat flux supplied (Fig. 4) with the available data [11] on bubble boiling of nitrogen in a large enclosure, which have been described quite well by the Kutateladze relation, shows that there is also bubble boiling in the porous wick structure, although the heat-removal intensity on the copper-fiber wick is larger than on a smooth surface. This is explained by the fact that metal-fiber wicks with a large housing thermal conductivity due to good contact with the heat-supply surface intensify the heat transfer, and, consequently, the heat-removal process with boiling proceeds both on the wall of the heat-pipe shell and also on the fibers inside the porous volume of the copper-fiber wick.

A characteristic feature of the heat pipes investigated is that they can transmit considerable heat fluxes at positive inclination angles, even when working with liquids such as nitrogen, because of the high transfer characteristics of the porous structure of the wick (permeability and effective pore size). For example, heat pipe No. 3 transmitted a heat flux of 11 W when working against gravity at an angle of 30°.

NOTATION

σ, surface-tension coefficient; r, latent heat of vaporization; ν, kinematic viscosity; λ, thermal conductivity; Π, porosity; D, pore size; d, outer diameter of shell; δ, thickness; L, length; K, permeability; Q, heat flux; T, temperature; φ, angle of inclination of heat pipe; Ω, mass of heat-transfer agent; $\Delta\Omega$, mass of excess

of heat-transfer agent; F, area of cross section; V, volume; α, heat-removal coefficient; q, heat-flux denxity. Indices: h, heater; c, condensation; T, transport; w, wick; eff, effective; t, theory, ex, experimental; wall, wall.

LITERATURE CITED

1. P. Brennan, ASME Paper 71-WA/HT-42 (1971).
2. A. Basiulis, ASME Paper 71-AV-29 (1971).
3. J. L. Thurman, J. Spacecraft Rockets, 6, 3 (1969).
4. M. Groll', Inzh.-Fiz. Zh., 28, No. 1 (1975).
5. B. F. Armaly, ASME Paper 71-WA/HT-28 (1971).
6. P. Joy, ASME Paper 70-HT/SPT-7 (1970).
7. L. L. Vasil'ev, Inzh.-Fiz. Zh., 28, No. 1 (1975).
8. M. G. Semena et al., Teplofiz. Vys. Temp., 13, No. 1 (1975).
9. M. G. Semena et al., Inzh.-Fiz. Zh., 31, No. 4 (1976).
10. J. H. Cosgrove, J. Nucl. Energy, 21, 547 (1967).
11. D. A. Clark, in: Advances in Heat Transfer [Russian translation], Mir, Moscow (1971), p. 361.

HEAT TRANSFER IN A TOROIDAL VESSEL PARTLY FILLED WITH LIQUID

Yu. A. Kirichenko and Zh. A. Suprunova

UDC 536.242

Measurements are reported on heat transfer for a toroidal vessel partly filled with liquid oxygen, nitrogen, or hexane for a constant heat-flux density at the boundary.

Long-term storage of cryogenic liquids has made it necessary to study processes due to external heat leaks that occur in vessels filled with such liquids. The final result from such studies should be recommendations on calculating the temperature distribution and pressure increase in such a vessel.

Here we report studies on the heat transfer in a toroidal vessel filled with liquid oxygen, nitrogen, or hexane for a constant heat-flux density at the casing.

The measurements were made on two toroidal vessels in which the small and large radii of the toroids were, respectively, $r_1 = 0.072$ m, $r_2 = 0.125$ m and $r_1 = 0.096$ m, $r_2 = 0.175$ m; the major process parameters were varied over the following ranges: heat-flux density $q = 15\text{-}300$ W/m^2; reduced initial temperature $T_0/T_c = 0.46\text{-}0.64$; and liquid filling factor $m = V_l/V = 0.17\text{-}0.90$. The working technique has previously been described [1].

The process occurs in the following sequence [2, 3]. When the heat flux begins to be supplied to the wall–liquid boundary, we obtain a boundary layer within which the liquid moves along the heated wall upward to the phase interface. The rising currents produce eddies near the surface of the liquid, which involve downward liquid flow. The flow is closed within the body of the liquid. The time τ_* needed to produce the first closed cycle has been interpreted [3] as the time needed to complete stage I (the internal transitional state). We now consider the details of the temperature distribution for each of the successive states. Figure 1 shows the temperature difference between the free surface and the lower region of uniform temperature as a function of time, $\vartheta_s - \vartheta_0 = f(\tau)$; the initial section is close to linear, while the latter section follows the law $\vartheta_s - \vartheta_0 \sim \tau^{0.5}$, which is ultimately followed by a horizontal part. Figure 1a shows that the rate of development of the temperature differential decreases as time passes. A comparison has been made [4] of the time for transition from the linear part $\vartheta_s - \vartheta_0 = f(\tau)$ to the $\vartheta_s - \vartheta_0 \sim \tau^{0.5}$ part with the time τ_* [3]. The relationship between these times indicates that the instant of transition from the linear part of $\vartheta_s - \vartheta_0 = f(\tau)$ to $\vartheta_s - \vartheta_0 \sim \tau^{0.5}$ represents the boundary between modes I and II, namely, τ_*. The instant τ_{**} of transition from $\vartheta_s - \vartheta_0 \sim \tau^{0.5}$ to $\vartheta_s - \vartheta_0 = \text{const}$ can be considered as the boundary between states II and III, which corresponds to the onset of a quasistationary state.

Cryogenic Technical-Physics Institute, Academy of Sciences of the Ukrainian SSR, Khar'kov.

Translated from Inzhenerno-Fizicheskii Zhurnal, Vol. 35, No. 1, pp. 54-61, July, 1978. Original article submitted June 17, 1977.

0022-0841/78/3501-0801$07.50